

# OPTIMIZATION OF LASER BEAM WELDING PARAMETERS FOR 90/10 CUPRONICKEL ALLOY WELDS USING TAGUCHI METHOD

MADDILI Praveena Chakravarthy<sup>1\*</sup>, DAKARAPU Santha Rao<sup>2</sup>

<sup>1\*</sup> Hindustan Shipyard limited, Visakhapatnam, Andhra Pradesh, India,  
e – mail: chakravarthymp@rediffmail.com

<sup>2</sup> Godavari Institute of Engineering and technology (Autonomous), Rajahmundry, Andhra Pradesh, India

**Abstract:** This study is to identify the most important control elements that will result in improve the tensile strength of Laser Beam Welded Cu-Ni 90/10 alloy joints. The different laser welding process parameters and levels were used for joining of Cu-Ni alloy. The process parameters like Laser Power (LP), Shielding Gas (argon) (SG), Focal Position (FP), & Welding Speed (WS) were chosen in the experimental study. The welding was carried on 4mm thick plate as per Taguchi's experimental design. The mechanical properties were evaluated and microstructural observations were carried out. It was discovered that highest tensile strength of 234 MPa & hardness of 83 Hv were obtained which has 90 % and 87 % of the base material. The most influential optimal process parameters were determined using S/N analysis and the percentage contribution of each process parameter was estimated using ANOVA. It was found that laser power was influential parameter with a 64 % contribution in obtaining highest strength of laser welded joints. The experimental values and the results of the confirmation experiments were in good agreement.

**KEYWORDS:** Laser beam welding (LBM), Copper–nickel (Cu–Ni) 90/10 alloys, Tensile strength (TS), Hardness, Design matrix and Taguchi method.

## 1 Introduction

Typical applications for copper-nickel alloys (Cu–Ni) include ship hulls, desalination plants, heat exchanger equipment, oil rigs and platforms, seawater and hydraulic pipelines, fish farming cages, used in chemical environments, seawater intake screens etc. because of their superior corrosion resistance. Arc welding of Copper alloys, such as GTAW and GMAW, is a difficult process. The most commonly encountered challenges in welding Cu-Ni alloys have been recognised defects like cracks, porosity, undercuts [1,2]. Due to fine and uniformly distributed grains in the weld region, mechanical properties of magnesium alloy welds improved as a result of the effect of LBW process parameters LP (2.5kw), WS (5.5 m/min), and FP (21.5 mm) [3]. The Cu-Ni alloy laser welds with LP(3.5kw) and WS(1.5 m/min) showed equiaxed, fine, and uniformly distributed grains at weld zone and exhibited better mechanical properties [4]. An ideal combination of laser parameters LP(1.6 kw), beam travel speed (0.25 - 1 cm/s), FP and SG (argon), resulted in good welding of V-Cr- Ti sheets (4mm thk) [5]. Recent research was conducted on materials like Mg, Cu, Al, Ti alloys, & SS by using LBW for improvement of mechanical properties [3-10].

The Taguchi approach was used for welding dissimilar stainless-steel (AISI 316) and low carbon steel plates (AISI 1009) by optimising weld parameters like LP, WS and FP in terms to reduce the fusion zone [11]. The orthogonal arrays and utility concept of Taguchi method were used to examine the optimization of laser process parameters like LP, FP, and WS. According to the analysis of variance, the optimization of various performance characteristics were

influenced by parameters like WS, LP and FP [12]. LBW parameters such as LP, WS, and FD for austenitic stainless steel and low carbon steel materials, as well as polypropylene-clay nanocomposite sheets with nano clay were optimised using Taguchi. The results showed that when clay content and welding speed increased, weld strength decreased, whereas with the increase in laser power, weld strength improved. In addition, as the focal location was increased, the weld strength increased and eventually decreased. Good mechanical characteristics were also obtained [13-14]. The combined Taguchi-response surface technique was used to improve laser welding parameters, and at LP (1344.73 W), WS (30 mm/s), FP (-2 mm), SG flow (30 L/min) the best quality welds were discovered, and improving mechanical qualities [15]. Optimising laser parameters by Taguchi method like LP, WS, FP, and SG flow rate for joining dissimilar material like 304 stainless steel to PMMA, titanium alloy plates, Al-Mg alloy welds, magnesium alloy welds, thin titanium shells, exhibited higher joint quality [16-22]. By using the Taguchi approach, welding parameters were optimized such as LP at 80w, WS at 400 mm/min, and FP at 0 mm, which had the biggest impact on the S/N ratio, influenced average penetration depth to width, and enhanced mechanical properties [23-24]. Using S/N ratio analysis and ANOVA, the best combination of process parameters which included LP (2.4 KW), WS (3m/min), and wire feed rate of 2m/min were found for minimum weld bead geometry [25].

## 2 Materials and methods

### 2.1 Materials

90/10 Cu-Ni alloy was used for joining of 4 mm thick plates and edges beveled at a 25° angle. The chemical composition of the alloy was determined by Spectrometric tracing of chemical elements which are listed in Table 1. The pieces are cut into 50 mm x 50 mm and edges were cleaned with chemical solvent of acetone.

Table 1 90/10 Cu-Ni alloy chemical compositions.

Ni	Mn	Fe	Zn	P	Pb	C	S	Others	Cu
10.9	0.64	1.3	0.03	0.06	0.04	0.04	0.03	0.15	Rest

### 2.2 Selection of process parameters

The process parameters and their levels were chosen in the welding process depending on the literature and the trial experiments. The process parameters comprise of laser power, shielding gas (argon), focal position, and welding speed. MINI Tab 18 was used to create the L16 matrix, which were presented in Table 2.

Table 2 Process parameters and their levels in laser welding

Welding parameters	Level 1	Level 2	Level 3	Level 4
Laser Power (kw)	2.0	2.5	3.0	3.5
Shielding Gas (argon)(Lit/min)	15	20	25	30
Focal Position (mm)	0	-1.0	-1.5	-2.0
Welding Speed (mm/min)	0.5	1.0	1.5	2.0

The work pieces were held firmly on the fixture by facing each other with a constant root gap of 0.1 mm. The two-pass welding was done for preparation of butt joints. The sixteen experiments were made as the design matrix with combination of process parameters. Fig. 1(a, b) shows the face & root of laser weld bead of 90/10 Cu-Ni alloy welds, respectively. The macroscopic observations was done and found no macro defects, the samples were cut in the transverse direction for estimation of mechanical properties like test tensile strength, hardness, bend strength and microstructural observations. As per ASTM E08 standards, the tensile

specimen were cut. For hardness testing and microstructure, a sample of 10 mm x 10 mm was taken in the centre of the joint. Figures 2(a, b, c) shows UTM, hardness testing machine and Laser welding set up.

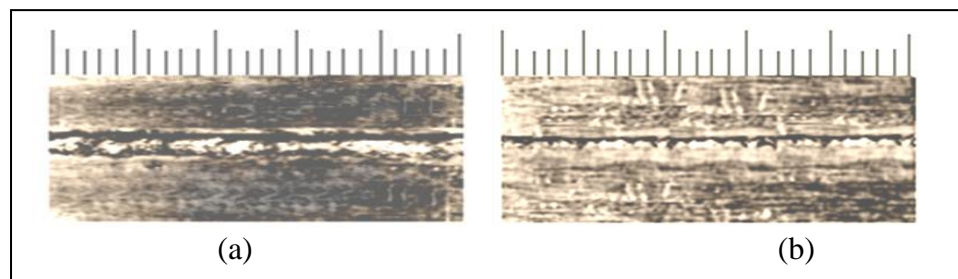


Fig. 1 (a) Weld face and (b) Root of Cu-Ni 90/10 laser welds

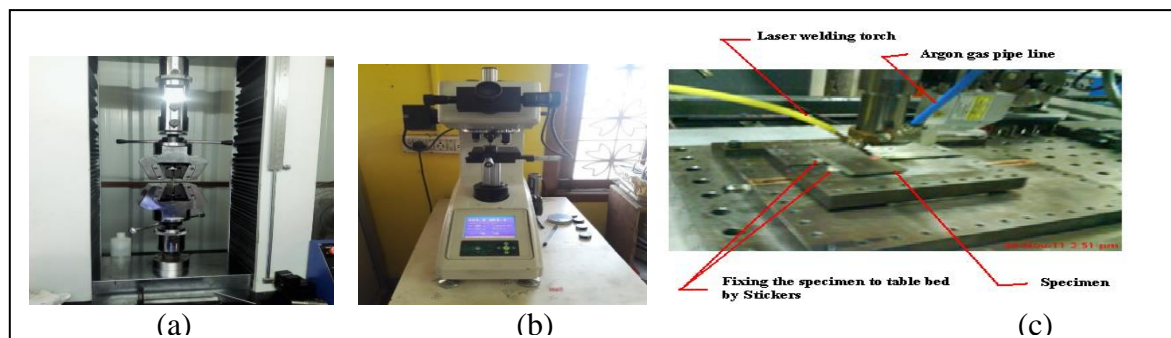


Fig. 2 (a) Computer controlled UTM, (b) Micro Vickers hardness testing machine, and (c) Laser welding set up.

### 2.3 Statistical analysis (taguchi) for optimization of process parameters

The ultimate tensile strength (UTS) of output response was studied to regulate the optimal process settings. For each factor, the effect of each parameter on S/N ratio, means, and response can be computed. Signal denotes the desired output characteristic, whereas noise denotes the unwanted output characteristic. In order to compute the maximal response, S/N ratio is chosen depending on the premise that the larger the better.

$$S/N \text{ ratio} = -10 \log (1/n \cdot \sum 1/y^2)$$

The observed data is taken as  $y$ . S/N ratio of all observations were calculated using MINI TAB as shown in Table.3. The output characteristic of the joint is the tensile strength. The contribution of laser power to good joint strength is ranked first in the response table for the S/N ratio, while focal location, welding speed, and shielding gas are ranked second, third, and fourth, respectively. A similar tendency was observed in the response table of mean as shown in Table 4, shows a similar tendency. Table 3 shows the S/N tensile strength ratio for each parameter at all levels.

The ANOVA results for TS (tensile strength) (means) are indicated in Table 5. Furthermore, the Fisher F-test can be used to evaluate which factors have a major impact on tensile strength. When  $F$  is large, a change in the welding parameter has a strong impact on the quality characteristics.

Table 3 Experimental results and S/N ratio

Experiment	LP (kw)	SG( argon) L/min	FP (mm)	WS (mm/min)	Ultimate Tensile strength (Response) (Y) MPa	S/N ratio dB
1	2.0	15	0.0	0.5	256.72	48.1892
2	2.0	20	-1.0	1.0	262.10	48.3693
3	2.0	25	-1.5	1.5	263.13	48.4034
4	2.0	30	-2.0	2.0	262.13	48.3703
5	2.5	15	-1.0	1.5	265.22	48.4721
6	2.5	20	0.0	2.0	265.20	48.4715
7	2.5	25	-2.0	0.5	263.20	48.4057
8	2.5	30	-1.5	1.0	276.77	48.8424
9	3.0	15	-1.5	2.0	276.45	48.8323
10	3.0	20	-2.0	1.5	282.16	49.0099
11	3.0	25	0.0	1.0	275.77	48.8109
12	3.0	30	-1.0	0.5	272.36	48.7029
13	3.5	15	-2.0	1.0	272.11	48.6949
14	3.5	20	-1.5	0.5	276.41	48.8311
15	3.5	25	-1.0	2.0	265.82	48.4918
16	3.5	30	0.0	1.5	265.55	48.4829

Table 4 Mean Response table for S/N ratio and experimental data for means

Level	S/N ratio				Experimental data for mean			
	LP	SG( argon)	FP	WS	LP	SG( argon)	FP	WS
1	48.33	48.55	48.62	48.53	261.0	267.6	269.9	267.2
2	48.55	48.67	48.72	48.68	267.6	271.5	273.2	271.7
3	48.84	48.53	48.51	48.59	276.7	267.0	266.4	269.0
4	48.63	48.60	48.49	48.54	270.0	269.2	265.8	267.4
Max-Min(Delta)	0.51	0.14	0.24	0.15	15.7	4.5	7.4	4.5
Rank	1	4	2	3	1	4	2	3

Table 5 ANOVA for TS (Mean) of LBW of Cu-Ni 90/10 alloy welds

Mean					
Parameter	Degree of Freedom	Adjusted sums of squares	Adjusted mean squares	Fisher (F) Value	% of contribution
LP	3	502.1	167.36	7.37	64.81
SG	3	47.88	15.96	0.85	6.18
FP	3	141.2	47.07	0.89	18.23
WS	3	51.96	17.32	0.29	6.71
Residual Error	3	31.52	10.50		4.07
Total	15	774.69			100.00

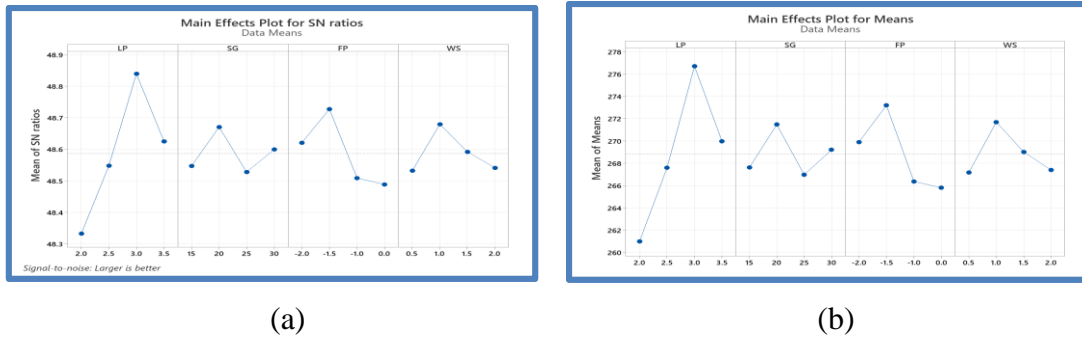


Fig. 3 Response plot comparison of (a) S/N ratio and (b) mean for tensile strength

The mean and S/N ratios for LP, SG, FP, and WS are graphed in Fig. 3, and the relevant values are tabulated. The best welding process parameters for tensile strength are based on the highest S/N ratio and mean values, with LP coming in first and FP coming in second. LP is determined to be the most important parameter, followed by FP. The SG (argon) has least effect on tensile strength of Cu-Ni 90/10 alloy joints. LP (3.0 KW), SG (argon) 20 L/min, FP (-1.5 mm), and WS (1.0 mm/min) are the best process parameters.

## 2.4 Predicting the optimum tensile strength

The optimum tensile strength can be predicted after determination of optimum process parameters using the following equation:

$$\bar{Y}_{\text{predicated}} = \bar{Y}_{\text{exp}} + (\bar{Y}_{\text{LP}} - \bar{Y}_{\text{exp}}) + (\bar{Y}_{\text{SG}} - \bar{Y}_{\text{exp}}) + (\bar{Y}_{\text{FP}} - \bar{Y}_{\text{exp}}) + (\bar{Y}_{\text{WS}} - \bar{Y}_{\text{exp}}) \text{ (or)}$$

$$\bar{Y}_{\text{predicated}} = \bar{Y}_{\text{LP}} + \bar{Y}_{\text{SG}} + \bar{Y}_{\text{FP}} + \bar{Y}_{\text{WS}} - 3 \times \bar{Y}_{\text{exp}}$$

Where  $\bar{Y}_{\text{predicated}}$  = Predicted Tensile strength

$\bar{Y}_{\text{exp}}$  = The total average response of the array's experiments,

$\bar{Y}_{\text{LP}}$  = Average responses for a LP L3,

$\bar{Y}_{\text{SG}}$  = Average responses for a SG L2,

$\bar{Y}_{\text{FP}}$  = Average responses for a FP L4,

$\bar{Y}_{\text{WS}}$  = Average responses for a WS L3.

$$\bar{Y}_{\text{exp}} = 4301.1 / 16 = 268.8188 \sim 268.82 \text{ MPa}$$

$$\bar{Y}_{\text{predicated}} = \bar{Y}_{\text{LP}} + \bar{Y}_{\text{SG}} + \bar{Y}_{\text{FP}} + \bar{Y}_{\text{WS}} - 3 \times \bar{Y}_{\text{exp}}$$

$$= 276.7 + 271.5 + 273.2 + 271.7 - 3 \times 268.82 = 286.64 \text{ MPa}$$

The predicted tensile strength was 286.64 MPa. To validate the model at the optimum setting of process parameters LP (3.0 kw), SG (argon) 20 L/min, FP (-1.5 mm), and WS (1.0mm/min), three confirmation experiments were conducted, which resulted an experimental average value of 278.13 MPa. The confirmation tests also conducted at optimal process parameters to validate the model and was found good agreement with the predicted value.

The contour plots for tensile strength of welded specimen are shown in Fig. 4(a, b, c). The detailed inferences are drawn from the taguchi optimization are validated using the contour plots. The Fig. 4(a) shows UTS can be improved with effect of LP (3.0 kw) and FP (-1.5 mm). The Fig. 4(b) shows UTS can be improved with effect of LP (3.0 kw) and WS (-1.0 mm/min). The Fig. 4(c) shows UTS can be improved with effect of LP (3.0 kw) and SG (20 L/min). Finally it is observed that laser power (LP) is the most influencing parameter in improvement of tensile strength.

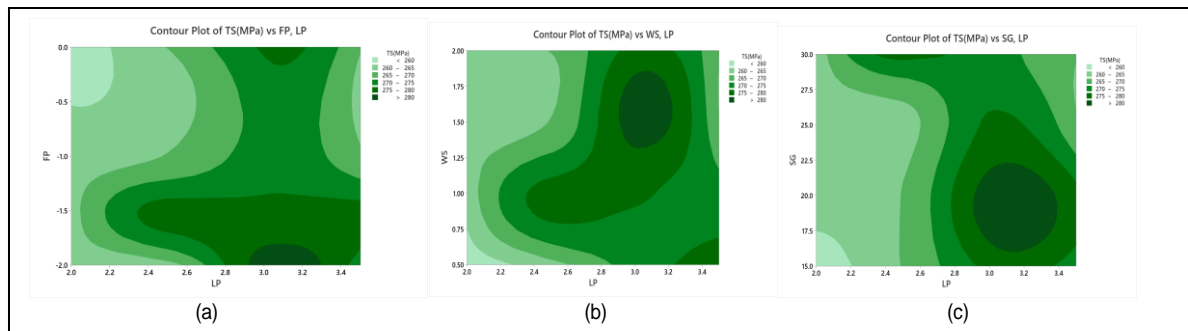


Fig. 4 (a) Contour on Laser Power vs Focal Position on UTS, (b) contour plot on Laser Power vs welding speed on UTS, (c) contour plot on Laser Power vs Shielding Gas on UTS

### 3 Results and discussion

#### 3.1 Results and discussion

The tensile test consists of a specimen that is grasped at each end by a tensile test machine gripper and subjected to tensile load. The tensile samples before and after the test was shown in the Fig. 5(a-b) and found that all samples were failed within the gauge portion only. The tensile strengths were plotted in the bar chart which is shown in the Fig.6 (a). The highest value of tensile strength of 282.16 MPa was obtained with laser power of 3 KW , gas flow of 20 litres /min with negative focal position of 2.0 mm and welding speed of 1.5 mm/min ( sample 10) which has 90.72 % of base material. Similarly the lowest value of tensile strength of 256.72 MPa was obtained with laser power of 2 KW , gas flow of 15 litres /min with zero focal position and welding speed of 0.5 mm/min(sample 1) which has 72 % base material tensile strength (311 MPa). Higher mechanical characteristics may be due to minimum weld bead shape, equiaxed fine grains, equally distributed, and extremely fine strengthening precipitates in the weld zone (hardness and tensile strength). The similar type of observations were reported by the researchers of [3, 10, 18, 20]. It also found that laser power has more influential parameters for higher strength of joints from the combination of process parameters.

The heat effected zone was very less when laser beam was used for joining of materials. When laser welds at sample 10 were compared to laser welds at other samples.

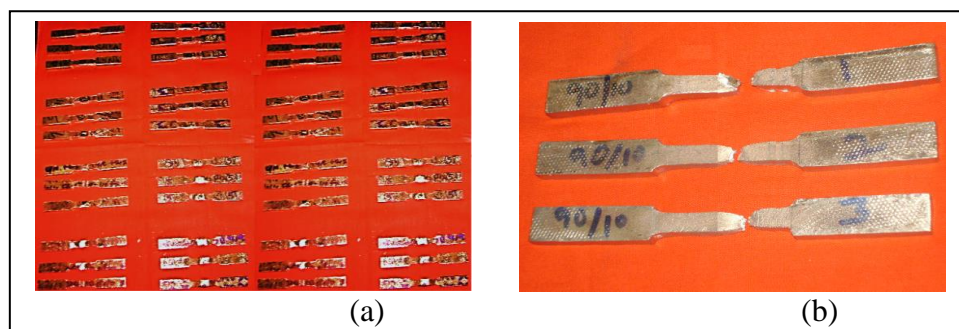


Fig.5 (a) L16 matrix tensile samples (average of 03 samples) before fracture and (b) after fracture (average of 03 samples)



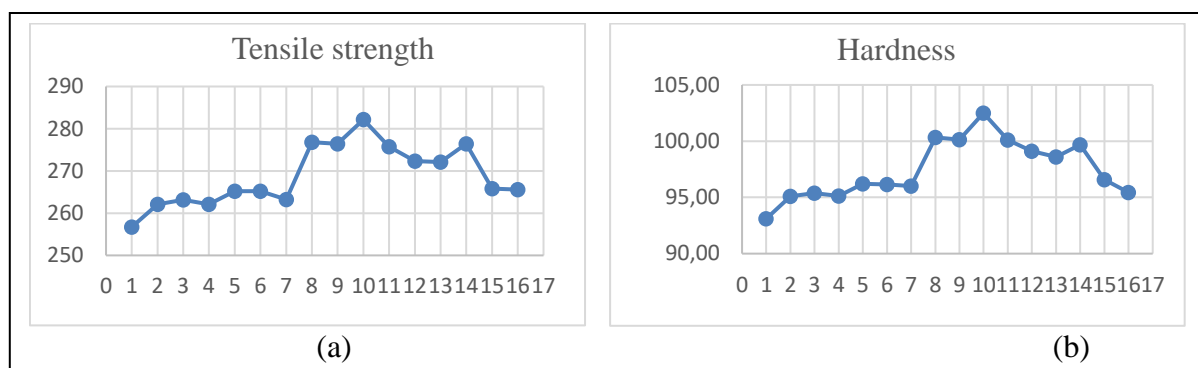


Fig. 6 (a) Results of Tensile strength of samples (b) Results of Hardness of welded samples

### 3.2 Micro-hardness Test

The micro Vickers hardness was measured in the weld zone by micro Vickers hardness testing machine in Fig. 2 (b). Five average hardness values were taken as per sample. Measurements were taken along the transverse direction at every 2 mm intervals from the centre line to either side of the weld to determine the weld's hardness. Fig. 6 (b) shows the average hardness values plotted and graphed. The hardness of base material (110 Hv) was higher than all welded specimen. Sample 10 obtained the highest value of 102.5 Hv. Cu and Ni particles are uniformly distributed throughout the weld zone, sample 10 exhibited the highest hardness of 102.5 Hv in the fusion zone, and this was indeed a reason for improved tensile qualities over other joints. The lowest hardness was Sample 1, which measured a hardness of 93.10 Hv.

### 3.3 Micro structural analysis

The specimens were taken from weld zone and polished with emery papers (320, 400, 600, 800, and 1000 and also polished with diamond paste. The mixture of nitric acid and glacial acetic acid in equal proportions were used for etching on the polished surfaces and then dried for 20 seconds. A SEM was used to determine the shape of the weld bead, width of face and root of welds. The fractography analysis was carried out with scanning electron microscope. It was observed that fine, equiaxed, and evenly dispersed grains were seen in LBW of Cu-Ni 90/10 welds. The energy dispersive spectroscopy (EDS) analysis were used to assess the chemical composition of weld metals.

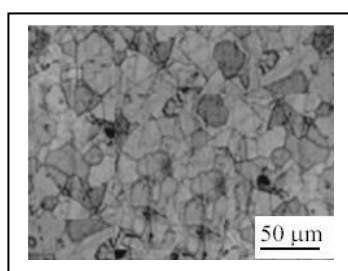


Fig. 7. Cu-Ni 90/10 alloy Base Metal

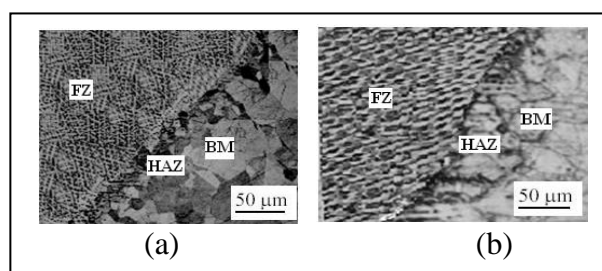


Fig. 8. Microstructures of Cu-Ni 90/10 alloy welds at HAZ (a) Sample 10 (b) Sample 1

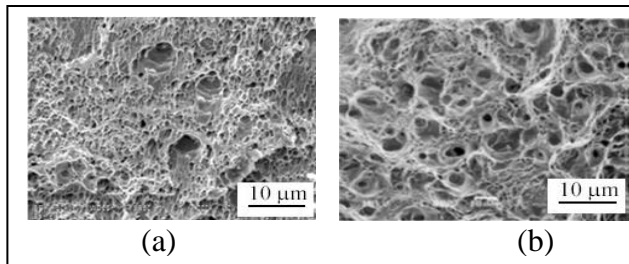


Fig. 9 SEM image of (a) sample 10  
(b) sample 1

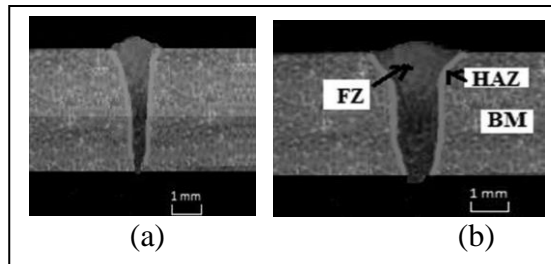
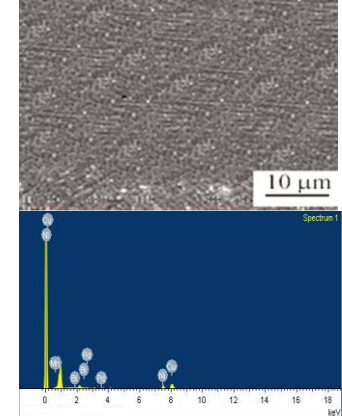
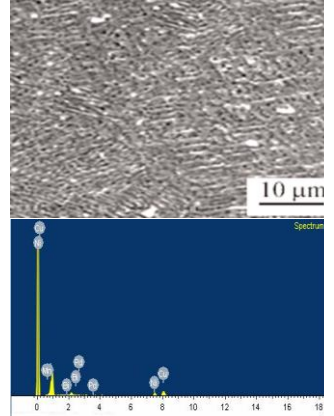


Fig. 10 Optical macrograph of transverse sections obtained for (a) Sample 1 and  
(b) Sample 10

 <table border="1" data-bbox="327 1041 646 1310"> <thead> <tr> <th>Metal</th><th>% Weight</th></tr> </thead> <tbody> <tr> <td>Copper</td><td>89.90</td></tr> <tr> <td>Nickel</td><td>9.90</td></tr> <tr> <td>Zinc</td><td>0.10</td></tr> <tr> <td>Manganese</td><td>0.20</td></tr> <tr> <td>Sum</td><td>100.00</td></tr> </tbody> </table>	Metal	% Weight	Copper	89.90	Nickel	9.90	Zinc	0.10	Manganese	0.20	Sum	100.00	 <table border="1" data-bbox="949 1041 1252 1310"> <thead> <tr> <th>Metal</th><th>% Weight</th></tr> </thead> <tbody> <tr> <td>Copper</td><td>89.89</td></tr> <tr> <td>Nickel</td><td>8.99</td></tr> <tr> <td>Zinc</td><td>0.92</td></tr> <tr> <td>Manganese</td><td>0.20</td></tr> <tr> <td>Sum</td><td>100.00</td></tr> </tbody> </table>	Metal	% Weight	Copper	89.89	Nickel	8.99	Zinc	0.92	Manganese	0.20	Sum	100.00
Metal	% Weight																								
Copper	89.90																								
Nickel	9.90																								
Zinc	0.10																								
Manganese	0.20																								
Sum	100.00																								
Metal	% Weight																								
Copper	89.89																								
Nickel	8.99																								
Zinc	0.92																								
Manganese	0.20																								
Sum	100.00																								
Fig. 11 EDS analysis of sample 10	Fig. 12 EDS analysis of sample 1																								

Base metal (Cu-Ni 90/10 alloy) microstructure has been taken by using Optical microscopy shown in Fig.7. The tensile fracture of sample 1 shown in Fig. 9(b) using SEM fractography revealed deep dimples and voids of varied sizes, this shows that the fracture is less ductile and resulted in lower mechanical properties compared to sample 10 shown in Fig. 9 (a). Microstructures of Sample 10 shown in Fig. 8 (a) and 10 (a) revealed good depth of penetration, less HAZ and bead width compared to microstructures of sample 1 shown in Fig. 8 (b) and 10 (b). As a result, sample 10 has superior mechanical properties to the other samples.

Due to proper melting and joining of weld metal with influence of laser power parameter of LBW as shown in SEM-EDS values at Fusion Zone (FZ) in Fig. 11 & 12, Sample 10 joint exhibited high percent of Cu & Ni, less percent of Zn and fine grains in FZ, resulting in superior mechanical properties than Sample 1.

## CONCLUSION

Laser Beam Welding was used to successfully weld the butt joints of Cu-Ni 90/10 alloys. The mechanical qualities of the joints were improved. The highest tensile strength and hardness, respectively of 278.13 MPa and 102.0Hv. The highest strength and hardness because of weld penetration due to laser power effect.



Taguchi optimization was used to optimise the process parameters, and it was discovered that laser power plays an important role in improving weld strength. LP (3.0 kw), SG (argon) 20 L/min, FP (-1.5 mm), and WS (1.0 mm/min) are the best process parameters. The predicted tensile was 286.64 MPa and confirmation experiments also conducted and found that error less than the 5% between the predicted and optimal experimental results. It concluded that model is valid for determination of optimal process parameters to obtain better mechanical properties.

## REFERENCES

- [1] "Copper-nickel fabrication", Copper Development Association (CDA), CDA Publication, **1999**. p. 139 <http://www.copperinfo.co.uk/alloys/copper-nickel/downloads/pub-39-copper-nickel-fabrication.pdf>
- [2] Devletian, J.H., Sullivan, M.J. "Flux cored arc welding of Cu-Ni 90/10 piping with Cu-Ni 70/30 filler metal. **2006**. [http://www.nsrp.org/3-RA-Panel\\_Final\\_Reports/2004\\_Flux\\_Cored\\_Electrode\\_Final\\_Report.pdf](http://www.nsrp.org/3-RA-Panel_Final_Reports/2004_Flux_Cored_Electrode_Final_Report.pdf)
- [3] Padmanaban, G., V. Balasubramanian, V. "Effects of laser beam welding parameters on mechanical properties and microstructure of AZ31B magnesium alloy", Transactions of Nonferrous Metals Society of China 21 (9), pp. 1971 – 1924, **2011**. DOI: 10.1016/S1003-6326(11)60950-3
- [4] Chakravarthy, M. P., Ramanaiah, N, Sundara Siva Rao, B. S. K. "Effect of laser welding on mechanical properties of 70/30 Cu-Ni alloy welds", Proc IMechE Part B: J Engineering Manufacture 228 (9), pp. 1153 – 1161, **2014**. DOI: 10.1177/0954405413517386
- [5] Reed, C. B., Natesan, K., Xu, Z., Smith, D. L. "The effect of laser welding process parameters on the mechanical and microstructural properties of V-4Cr-4Ti structural materials", Journal of Nuclear Materials, 283 – 287 (2), pp. 1206 – 1209, **2000**. DOI: 10.1016/S0022-3115(00)00348-2
- [6] Dutta Majumdar, J., Manna, I. "Laser processing of materials", Sadhana 28, pp. 495 – 562, **2003**. DOI: 10.1007/BF02706446
- [7] Akman, E., Demir, A., Canel, T., Sınmazcelik, T. "Laser welding of Ti6Al4V titanium alloys", Journal of materials processing technology 209 (8), pp. 3705 – 3713, **2009**. DOI: 10.1016/j.jmatprotec.2008.08.026
- [8] Kabir, A. S. H., Cao, X., Medraj, M., Wanjara, P. Cuddy, J. Birur, A. "Effect of welding speed and defocusing distance on the quality of laser welded Ti-6Al-4V", Materials Science and Technology (MS&T), Laser Application in Materials Processing, Houston, Texas, pp. 2787 – 2797, **2010**.
- [9] El-Batahgy, A., Kutsuna, M. "Laser beam welding of AA5052, AA5083 and AA6061 aluminum alloys", Advances in Materials Science and Engineering 2009, **2009**. DOI: 10.1155/2009/974182
- [10] Jun, Y., Ming, G., Xiaoyan, Z. "Study on microstructure and mechanical properties of 304 stainless steel joints using TIG, laser and laser TIG hybrid welding", Optics and Lasers in Engineering 48 (4), pp. 512 – 517, **2010**. DOI:10.1016/j.optlaseng.2009.08.009
- [11] Anawa, E. M., Olabi, A. G. "Using Taguchi method to optimize welding pool of dissimilar laser-welded components", Optics & Laser Technology 40 (2), pp. 379 – 388, **2008**. DOI:10.1016/j.optlastec.2007.07.001
- [12] Duradundi, S. B., Krishna, S. P., Buvanashakaran, G. "Parameter optimization of laser transformation hardening by using Taguchi method and utility concept", Int J Adv Manuf

Technol 52, pp. 1067 – 1077, **2011**. DOI:10.1007/s00170-010-2787-z

- [13] Prabakaran, M. P., Kannan, G. R. “Optimization of laser welding process parameters in dissimilar joint of stainless steel AISI316/AISI1018 low carbon steel to attain the maximum level of mechanical properties through PWHT”, Optics and Laser Technology, 112, pp. 314 – 322, **2019**. DOI: 10.1016/j.optlastec.2018.11.035
- [14] M. R. Nakhaei, N. B. Mostafa Arab, and M. Hoseinpour Gollo, Experimental study on optimization of CO2 laser welding parameters for polypropylene-clay nanocomposite welds, Journal of Mechanical Science and Technology 27 (3) (2013) 843~848. DOI 10.1007/s12206-013-0109-8
- [15] Jiangqi, L., Wenhao, H., Jiawei, X., Zhengwei, M. “Parameter optimization of laser welding of steel to Al with pre-placed metal powders using the Taguchi-response surface method”, Optics and Laser Technology 108, pp. 97 – 106, **2018**. DOI: 10.1016/j.optlastec.2018.06.026
- [16] Lung, K. P., Che, Ch. W., Shien, L. W., Hai, F. S. “Optimizing multiple quality characteristics via Taguchi method-based Grey analysis”, Journal of Materials Processing Technology 182 (1 – 3), pp. 107 – 116, **2007**. DOI: 10.1016/j.jmatprotec.2006.07. 015
- [17] Santha Rao, D., and Ramanaiah, N. “Process parameters optimization for producing AA6061/TiB2 composites by friction stir processing”. Strojnícky časopis – Journal of Mechanical Engineering 67 (1), pp. 101 – 118, **2017**. DOI: 10.1515/scjme-2017-0011
- [18] Yijie, H., Xiangdong, G. , Bo, M., Guiqian, L., Nanfeng, Z., Yanxi, Z., Deyong, Y. “Optimization of weld strength for laser welding of steel to PMMA using Taguchi design method”, Optics & Laser Technology 136, **2021**. DOI: 10.1016/j.optlastec.2020.106726
- [19] Sathiya, P., Abdul Jaleel, M. Y., Katherasan, D. “Optimization of welding parameters for laser bead-on-plate welding using Taguchi method”, Prod. Eng. Res. Devel. 4 (5), pp. 465 – 476, **2010**. DOI: 10.1007/s11740-010-0234-5
- [20] Basha, S. K., Raju, M. V. J., Kolli, M. “Multi-Objective Optimization of Process Parameters for Powder Mixed Electrical Discharge Machining of Inconel X-750 Alloy Using Taguchi-Topsis Approach”, Strojnícky časopis – Journal of Mechanical Engineering 71 (1), pp. 1 – 18, **2021**. DOI: 10.2478/scjme-2021-0001
- [21] Yan, J., Gao, M., Zeng, X. “Study on microstructure and mechanical properties of 304 stainless steel joints using TIG, laser and laser TIG hybrid welding”, Opt Laser Eng 48 (4), pp. 512 – 517, **2010**. DOI: 10.1016/j.optlaseng.2009.08.009
- [22] Bijivemula, N. R., Pothur, H., Chevireddy, E. R. “Mechanical and metallurgical characterisation of Co2 laser beam welding AISI 4130 and AISI 310 sheets of steel”, Strojnícky časopis – Journal of Mechanical Engineering 71 (2), pp. 19 – 30, **2021**. DOI: 10.2478/scjme-2021-0014
- [23] Xiansheng, N., Zhenggan, Z., Xiongwei, W., Luming, L. “The use of Taguchi method to optimize the laser welding of sealing neuro-stimulator”, Optics and Lasers in Engineering 49 (3), pp. 297 – 304, **2011**. DOI: 10.1016/j.optlaseng.2010.11.005
- [24] Lung, K. P., Che, Ch. W., Ying, Ch. H., Kye, Ch. H. “Optimization of Nd:YAG laser welding onto magnesium alloy via Taguchi analysis”, Optics & Laser Technology 37 (1), pp. 33 – 42, **2005**. DOI: 10.1016/j.optlastec.2004.02.007
- [25] Yang, D., Li, X., He, D., Nie, Z., Huang, H. “Optimization of weld bead geometry in laser welding with filler wire process using Taguchi’s approach”, Optics & Laser Technology 44 (7), pp. 2020 – 2025, **2012**. DOI: 10.1016/j.optlastec.2012.03.033